Title
Eddy covariance fluxes of peroxyacetyl nitrates (PANs) and NOy to a coniferous forest

Journal
Journal of Geophysical Research, 111(D9)

ISSN
0148-0227

Authors
Turnipseed, AA
Huey, LG
Nemitz, E
et al.

Publication Date
2006

DOI
10.1029/2005jd006631

Eddy covariance fluxes of peroxyacetyl nitrates (PANs) and NO_y to a coniferous forest

A. A. Turnipseed,[1] L. G. Huey,[2] E. Nemitz,[3] R. Stickel,[2] J. Higgs,[2] D. J. Tanner,[2] D. L. Slusher,[2,4] J. P. Sparks,[5] F. Flocke,[1] and A. Guenther[1]

Received 29 August 2005; revised 21 December 2005; accepted 26 January 2006; published 6 May 2006.

[1] We employed a fast response thermal dissociation-chemical ionization mass spectrometer (TD-CIMS) system to measure eddy covariance fluxes of peroxyacetyl nitrate (PAN), peroxypropionyl nitrate (PPN) and peroxymethacryloyl nitrate (MPAN). Fluxes were measured for eight consecutive days in July 2003 at a Loblolly pine forest in North Carolina along with eddy covariance NO_y fluxes. Covariances between PAN concentration and vertical wind velocity indicated consistent deposition fluxes that ranged up to approximately -14 ng N m^{-2} s^{-1}. The average daytime flux peaked at -6.0 ng N m^{-2} s^{-1} and accounted for $\sim$20% of the daytime NO_y flux. Calculations suggest minimum daytime surface resistances for PAN in the range of 70–130 s m^{-1}. It was estimated that approximately half of daytime uptake was through plant stomates. Average PAN deposition velocities, V_d(PAN), showed a daytime maximum of $\sim$10.0 mm s^{-1}; however, deposition did not cease during nighttime periods. V_d(PAN) was highly variable at night and increased when canopy elements were wet from either precipitation or dew formation. Diel patterns of deposition velocity of MPAN and PPN were similar to that of PAN. These results suggest that deposition of PAN, at least to coniferous forest canopies, is much faster than predicted with current deposition algorithms. Although deposition of PAN is unlikely to compete with thermal dissociation during warm summer periods, it will likely play an important role in removing PAN from the atmosphere in colder regions or during winter. The fate of PAN at the surface and within the plants remains unknown, but may present a previously ignored source of nitrogen to ecosystems.

Citation: Turnipseed, A. A., L. G. Huey, E. Nemitz, R. Stickel, J. Higgs, D. J. Tanner, D. L. Slusher, J. P. Sparks, F. Flocke, and A. Guenther (2006), Eddy covariance fluxes of peroxyacetyl nitrates (PANs) and NO_y to a coniferous forest, *J. Geophys. Res.*, *111*, D09304, doi:10.1029/2005JD006631.

1. Introduction

[2] Peroxyacyl nitrates (PANs) are important species in the atmosphere that are produced in the atmosphere by reaction (1f).

$$RC(O)OO + NO_2 \rightleftharpoons RC(O)OONO_2 \qquad (1f, 1r)$$

where R is a hydrocarbon group. The most abundant of these compounds is peroxyacetyl nitrate (PAN, R = CH_3). The lifetime of PAN and PAN-like compounds near the earth's surface is thought to be dominated primarily by thermal decomposition (1r) and subsequent reaction of the peroxyacetyl radical (PA) with NO [*Roberts and Bertman*, 1992], e.g.,

$$CH_3C(O)OO + NO \rightarrow CH_3C(O)O + NO_2 \qquad (2)$$

The reversible reaction (1f, 1r) is highly dependent on temperature [*Bridier et al.*, 1991] and, thus, leads to PAN's role as a temporary reservoir of NO_x (= NO + NO_2), compounds that are critical in tropospheric ozone production. PAN compounds are quite stable in the colder temperatures of the middle-upper troposphere and can be transported long distances at these altitudes. Subsequent downward mixing to the surface can cause the release of active NO_x in more rural or remote regions and play a large role in ozone formation in these regions [*Moxim et al.*, 1996; *Singh and Hanst*, 1981; *Cox and Roffey*, 1977].

[3] Losses of PAN (and other PAN-like compounds) via wet deposition have been considered relatively unimportant due to its small Henry's law coefficient under atmospheric conditions ($\sim$4.1 M atm^{-1} [*Kames and Schurath*, 1995]). This low solubility should also tend to inhibit dry deposition as well since many surface processes involve initial dissolution in aqueous solutions (i.e., within leaves, etc.). How-

[1]Atmospheric Chemistry Division, National Center for Atmospheric Research, Boulder, Colorado, USA.
[2]School of Earth and Atmospheric Sciences, Georgia Institute of Technology, Atlanta, Georgia, USA.
[3]Centre for Ecology and Hydrology (CEH), Penicuik, Midlothian, U.K.
[4]Department of Chemistry and Physics, Coastal Carolina University, Conway, South Carolina, USA.
[5]Department of Ecology and Evolutionary Biology, Cornell University, Ithaca, New York, USA.

0148-0227/06/2005JD006631

ever, a recent leaf-level study observed considerable uptake of PAN into leaf stomates of a wide variety of species, suggesting a possible significant atmospheric loss process [*Sparks et al.*, 2003]. This is also of interest from a biological standpoint, as PAN deposition may provide a source of nitrogen (usually a limiting nutrient in temperate forests) directly to vegetation.

[4] Previous studies on the dry deposition of PAN have produced varied results, with deposition velocities ($V_d \equiv -$Flux/[PAN]) ranging from 1–8 mm s^{-1} [*Hill*, 1971; *Garland and Penkett*, 1976; *Shepson et al.*, 1992a; *Schrimpf et al.*, 1996; *McFadyen and Cape*, 1999a; *Doskey et al.*, 2000, 2004]. These were primarily conducted over short canopies (grasslands or crops) and/or conducted at night when plant photosynthetic activity is negligible. The only study which reports daytime dry deposition fluxes is that of *Doskey et al.* [2000, 2004], who showed a small depositional flux (V_d = 1.3 ± 1.3 mm s^{-1}) which could not be explained by either cuticular plant uptake or by enhanced thermal decomposition on plant surfaces. They suggested that the primary uptake of PAN was through the stomates into the vegetation, consistent with the study of *Sparks et al.* [2003].

[5] In prior ecosystem-level studies, the deposition velocity was derived either indirectly from the exponential decrease in the PAN concentration during the night, referred to as the Boundary-Layer Budget technique [*Shepson et al.*, 1992a; *McFadyen and Cape*, 1999a] or from using gradient methods [*Schrimpf et al.*, 1996; *Doskey et al.*, 2004]. The Boundary-Layer Budget approach assumes that deposition is the only sink and that the evolution of the nocturnal boundary layer is understood. Gradient methods become more uncertain when: (1) the observed gradients are small relative to the precision of the measurements (as was the case in the *Doskey et al.* [2004] study), and (2) over tall canopies (such as forests) where gradient levels must often be located within the roughness sublayer for practical reasons. Here, profiles cease to be logarithmic and standard expressions for flux-gradient relationships are not applicable. In addition, large sweep-ejection air motions in the roughness sublayer can lead to counter-gradient transport, and subsequently cause an underestimate of the flux [*Cellier and Brunet*, 1992; *Simpson et al.*, 1998]. No similar deposition studies of other peroxyacyl compounds other than PAN have been reported to our knowledge.

[6] In this study, we have used the recently developed technique of thermal decomposition-chemical ionization mass spectroscopy (TD-CIMS) [*Slusher et al.*, 2004] coupled with sonic anemometry to measure fluxes of PAN by eddy covariance (EC). The TD-CIMS system has the capability of making reasonably precise concentration measurements of PAN with integration times of less than 0.3 s, thus making it suitable for the eddy covariance technique, especially above rough surfaces. We have also used this technique to measure deposition fluxes of peroxypropionyl nitrate (PPN, $CH_3CH_2C(O)O_2NO_2$) and peroxymethacryloyl nitrate (MPAN, $CH_2C(CH_3)C(O)O_2NO_2$). Eddy covariance has several advantages over previous studies in that this is a direct measure of the flux (it does not depend on the concept of similarity and measuring the flux of another scalar such as temperature) and is suitable for tall canopies. In addition to the PAN fluxes, concurrent NO_y (= NO + NO_2 + HNO_3 + NO_3^- + PANs) fluxes were conducted in order to ascertain the contribution of PAN, as well as PPN and MPAN, deposition to the total amount of gaseous oxidized nitrogen dry deposited to the ecosystem.

2. Experiment

2.1. Site Description

[7] The experiments were conducted at the Duke Forest FACE (Free Air CO_2 Enrichment) site at one of the control towers (i.e., no enhanced CO_2 levels). The site has been described in depth previously, both in terms of its physical and biological properties, and its suitability for measurement of ecosystem level fluxes by eddy covariance [*Katul et al.*, 1999]. Therefore we will present only a brief description here. The forest consisted of a 20 year old Loblolly pine (*Pinus taeda*) plantation with an average canopy height (h_c) of 17 m and an LAI of ~3.5 m^2 m^{-2} [*Katul et al.*, 1999]. The displacement height (d) was estimated as $0.7h_c$ = 11.9 m. The understory consisted of a smattering of hardwood species such as sweetgum (*liquidambar styraciflua*) and tulip poplar (*Liriodendron tulipfera*). The sweetgum was typically ≤10 m in height, although some of these trees did protrude into the upper canopy. Homogeneous vegetation in the direction of the primary wind direction (southwest) was ~1 km. Measurements were undertaken between July 13 and July 25th, 2003 (Day of Year 194–206) during the peak of the growing season.

[8] The site is located approximately 6 km northwest of Chapel Hill, NC and lies 1.5–2 km west of an interstate highway. Although the predominant winds are from the southwest, the site typically experiences moderate anthropogenic pollution, and can be impacted at times by these local sources.

2.2. Measurement Methodology

[9] Flux measurements were made from a scaffolding tower at a height of 26 m (~9 m above the canopy, $z - d$ = 14.1 m). Three dimensional wind velocities (u, v, w) were measured at 10 Hz by a 3-dimensional sonic anemometer (ATI-K, Advanced Technologies Inc., Boulder, CO) extended on a boom 1.5 m from western side of the tower. Fast temperature measurements (T_s) derived from the speed of sound were also recorded from the 3-D sonic anemometer allowing for the calculation of simultaneous sensible heat fluxes.

[10] The TD-CIMS instrumental setup is shown in Figure 1. Sample air was brought from the proximity of the sonic anemometer measurement path (~30 cm) at a high flow rate (>40 lpm) through a Teflon filter and then a 45 m, 3/8″ OD Teflon inlet line. The high flow rate ensured turbulent flow within the tube which minimizes axial mixing by minimizing the radial velocity profiles which would result in a loss of flux [*Lenschow and Raupach*, 1991]. It also minimized contact time between the sample gas and the tube walls as the residence time along this path was <3 s (see analysis in next section). A small portion (~1900 sccm) of the main flow was drawn into the TD-CIMS. The TD-CIMS technique and its comparison with more established chromatographic techniques was given in *Slusher et al.* [2004]. Briefly, the sample flow first passes through a 25 cm × 0.64 cm i.d. PFA (perfluoro

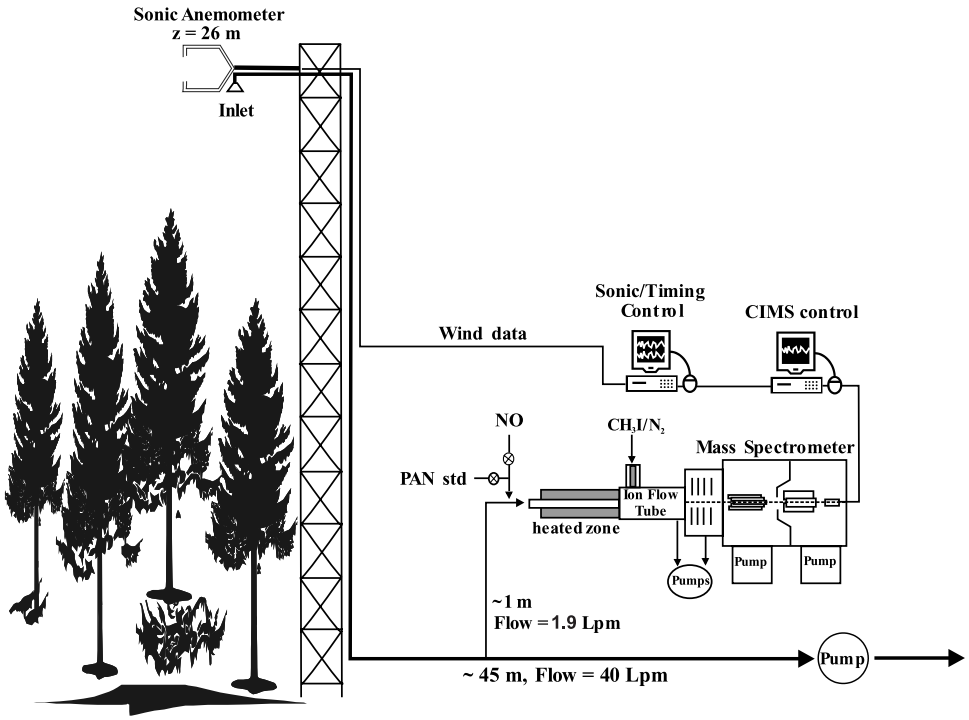

Figure 1. Schematic of the overall setup for the TD-CIMS system for measuring fluxes of PAN-compounds.

alkoxy alkane) Teflon tube heated to an external temperature of 180°C. This serves to efficiently dissociate peroxyacyl nitrates immediately via reaction (1r). This flow is then drawn through a 0.5 mm diameter orifice into a 10 cm-long, 4 cm i.d. flow tube maintained at ~20 Torr. I^- was synthesized in an ion source [*Slusher et al.*, 2004] and added to the flow tube in 2.5 slpm of nitrogen. Within the flow tube, peroxyacyl radicals react with I^- via:

$$RC(O)O_2 + I^- \rightarrow RC(O)O^- + IO \qquad (3)$$

where R stands for any organic group (for PAN, R = CH_3).

[11] A small portion of the flow tube effluent (ca. 50 sccm) is sampled into the collisional dissociation chamber (CDC), which dissociates weakly bound water clusters. The product and reagent ions are then concentrated and guided by an octopole into the quadrupole mass filter. The mass selected ions exiting the quadrupole were detected with a channeltron ion multiplier. Current pulses from the channeltron were counted and recorded by the computer every 250 ms and concurrently output to the computer recording the sonic data. During each 250 ms time period the signals at 59, 73 and 85 amu were monitored with approximately equal duty cycles. These masses correspond to the ions generated from PAN, PPN, and MPAN, respectively, via reaction (3). In general, PPN and MPAN were at much lower mixing ratios (<300 pptv) than PAN, thus leading to noisier flux calculations. During other times, mass spectra were recorded from 30 to 200 amu. These experiments provided a periodic quality check on the CIMS as well as a mechanism for identifying other PAN type compounds present in the moderately polluted forest air.

[12] Once every thirty minutes the PAN sensitivity and the background at all masses were measured. The instrument was zeroed by addition of a large excess of NO (1 ppm) (Scott-Marrin) to the inlet which effectively titrates the RC(O)OO radicals via reaction (2). The TD-CIMS was calibrated by standard addition of known amounts of PAN just upstream of the heated tube. PAN was generated from a photolytic source similar to that described by *Warneck and Zerbach* [1992] and the yield of PAN from this technique was assumed to be 93 ± 3% as determined in previous studies [*Slusher et al.*, 2004]. The sensitivity of the CIMS to PPN has been determined in laboratory experiments to be the same as for PAN [*Slusher et al.*, 2004]. However, the ratio of PAN to MPAN sensitivity has been shown to range from 3–10 (typically 8) depending on conditions [*Slusher et al.*, 2004; Swanson et al., manuscript in preparation]. For this work, the sensitivity of the CIMS to MPAN was assumed to be a factor of 8 less than that of PAN (Swanson et al., manuscript in preparation). It should be noted that this uncertainty affects the reported concentrations and fluxes but not the deposition velocities. Figure 2a shows an example of a standard addition of PAN, at the end of a calibration sequence, and gives an indication of the response time of the instrument to a step-change in PAN. As seen in the figure, this response is τ (1/e) < 0.3 s. As PAN was added to the entrance of the TD-CIMS, this response time does not include effects from the inlet line. Concurrent measurements using a proton-transfer mass spectrometer (PTRMS), sampling through the same inlet line, suggested only a small broadening of the time response due to axial diffusion within the tubing (T. Karl, personal communication).

[13] NO_y fluxes were measured similar to the method described by *Munger et al.* [1996]. Sample air at 2 slpm was passed through a small, 15 cm long, $^1/_4''$ OD piece of Pyrex tubing into a heated glass catalytic converter. The converter contained a 60-cm piece of $^1/_4''$ gold tube that was heated to 295°C. A small flow of H_2 (25 sccm) was added just prior

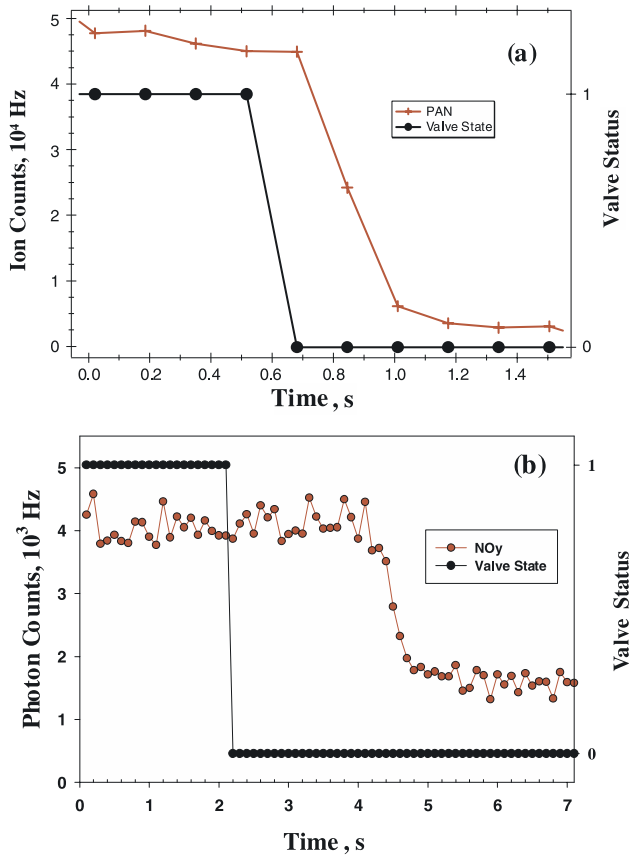

Figure 2. Time series showing the rapid shut-off of the calibration standard (PAN or NO) from the (a) TD-CIMS system and (b) the NO_y chemiluminescence system. Valve status = 1 when calibration standard is turned on, = 0 when off.

to the heated region to help reduce oxidized nitrogen species to NO. The flow was then passed through a mass flow controller and 10 m of $^1/_4''$ Teflon tubing to a NO analyzer (Model CLD 770, Ecophysics, Duernten, Switzerland). The CLD770 detects light from the chemiluminescent reaction between NO and O_3:

$$NO + O_3 \rightarrow NO_2 + O_2 + h\upsilon \quad (4)$$

Light emission was detected by a red-sensitive photomultiplier tube and the subsequent current pulses were amplified and counted directly by a PC and recorded at 10 Hz. The analyzer was periodically zeroed by diversion of the flow through a pre-reaction chamber where excess O_3 was added to consume NO before entering the reaction chamber. The instrument was calibrated daily by injecting a small flow (1–10 sccm) of a NO standard (1.9 ppm NO/N_2) at the inlet. Figure 2b shows a plot of the photon counts versus time when the NO standard was turned off by a solenoid just next to the inlet. These tests (conducted upon each calibration) indicated an adequately fast response ($\tau <$ 0.5 s, 1/e). Laboratory tests also indicated a conversion efficiency of unity for NO_2. The conversion efficiency of our NO_y system for HNO_3 was not determined as no calibrated source of gas phase HNO_3 was available.

[14] Other measurements taken during the campaign include standard meteorological variables (wind speed and direction, temperature, relative humidity, precipitation, incoming light, etc.) at both the measurement tower and the nearby (~250 m away in the same forest stand) Duke Forest Ameriflux site. CO_2 and H_2O vapor fluxes were also measured at the AmeriFlux tower. NO_x and O_3 were measured at a nearby tower above the canopy by either UV absorption (O_3) or by chemiluminescence (NO, NO_x) (Toohey, personal communication).

[15] The serial output from the ATI-K sonic anemometer was collected on a PC running an in-house LabView (National Instruments) program. Counts from the NO_y instrument were counted directly by this primary PC and synchronized with the wind velocity data at a rate of 10 Hz. Counts from the ion channeltron of the TD-CIMS were counted by a second PC and then a serial data stream was sent to the primary PC to be synchronized with the wind data at a rate of ~4 Hz to the nearest 10 Hz wind measurement. Any lag or slight time misalignment which may have arisen due to the transfer time between computers or difference in sampling rates was accounted for before flux calculations (see below) and would be expected to be small (1–2 samples) compared to the lag introduced by the inlet tubing. The averaging period for flux calculation for PAN, PPN and MPAN was 25 min. (with 5 min. of zeroing/calibration at the end of each period).

2.3. Eddy Flux Measurements and Validation

[16] Figure 3 gives an example of a typical time series observed during this study showing vertical wind velocity (w), sonic virtual temperature (T_s), PAN and NO_y. Significant anti-correlations can be observed between the fluctuations of PAN (as well as NO_y) and w. Stronger correlations can be observed with temperature as expected due to higher scalar-scalar covariances [*Lenschow*, 1995]. Prior to calculation of fluxes, the wind coordinate frame was rotated such that $\overline{v} = \overline{w} = 0$ [*Kaimal and Finnigan*, 1994]. Scalar time series were despiked, linearly detrended, and finally shifted in time relative to w to account for lags induced by inlet lines. These lags were determined from the maximum in the cross correlation between the vertical wind velocity, w, and the species of interest (e.g., PAN, NO_y). Figure 4a shows plots of the average cross correlation between both w and T_s with PAN derived for all of the time periods on July 19. These plots for each time period consistently indicated anti-correlation with w (deposition) with a peak at ~2.7 s, consistent with flow rate measurements and tubing lengths in the system. The same time lag was found for PPN and MPAN. NO_y cross correlations (data not shown) were similar showing consistent deposition and a lag of ~2.3 s.

[17] Fluxes were then calculated from the covariance between vertical wind velocity (w) and the species mixing ratio (c)

$$F = \rho\langle w'c'\rangle \quad (5)$$

Here, $\langle\ \rangle$ denote a time average, the primes denote fluctuations from the mean ($x' = x(t) - \overline{x}$, $\overline{x}$ = mean) and ρ is the mean atmospheric density. Corrections due to sensible heat [*Webb et al.*, 1980] were not applicable as the sample gas was heated to a constant temperature prior to

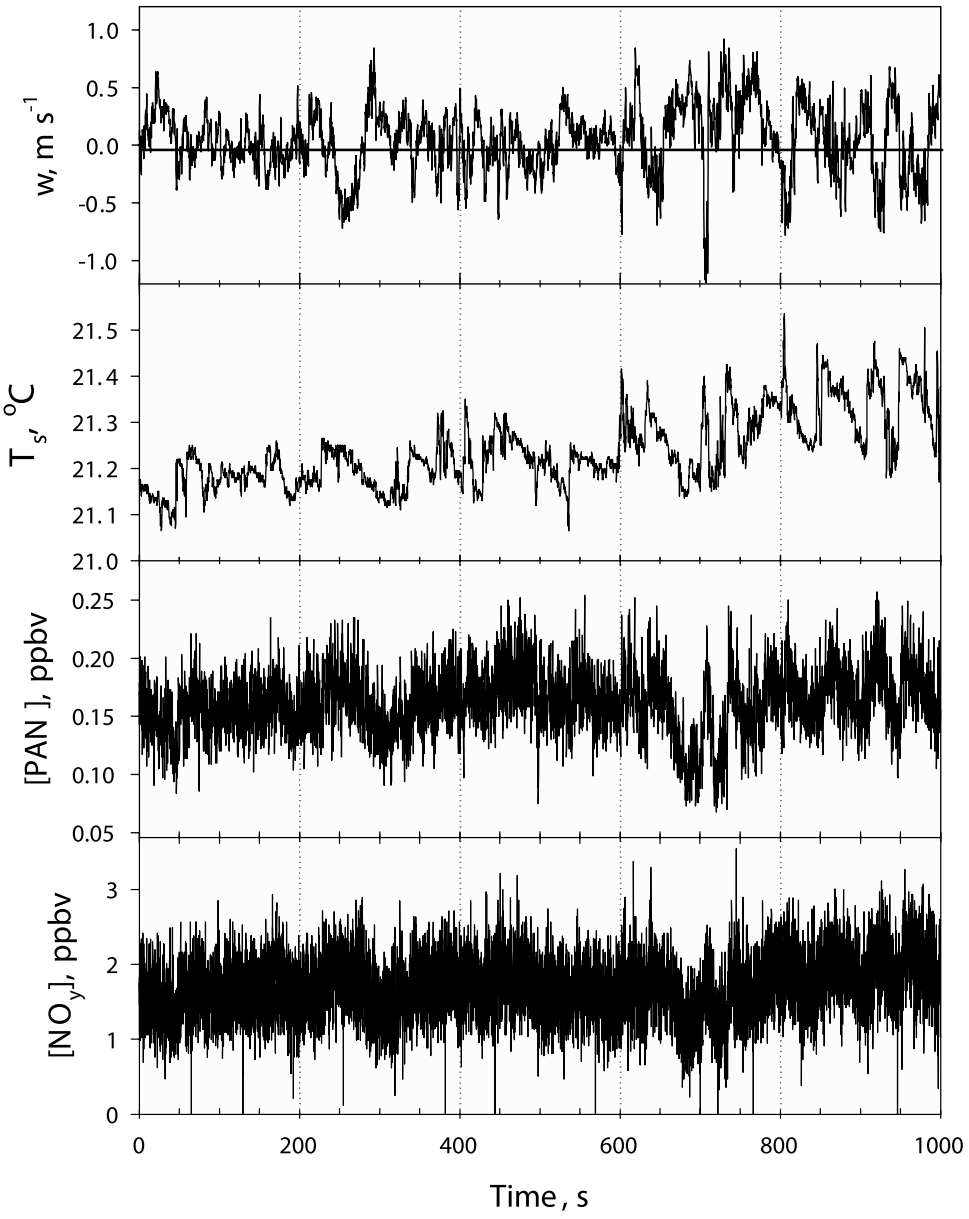

Figure 3. Time series of vertical wind velocity (w), sonic temperature (T_s), [PAN] and [NO_y] taken on July 19 beginning at 5:30 local standard time.

detection in both instruments. Similar corrections due to latent heat fluxes [*Webb et al.*, 1980] were not applied due to the poor temporal overlap between the measured quantities; however, when available, these corrections tended to be <2%. Correction due to instrument time response was accomplished by applying a low-pass filter to the sonic-derived T_s with a time constant of 0.5 s for both PAN (as well as PPN and MPAN) and NO_y (derived from data in Figure 2 and an estimate of the inlet broadening for PANs). Heat fluxes were then recomputed and compared to the fluxes calculated from the 10 Hz data to determine a flux correction factor for each species. These correction factors were typically <8% with smaller corrections during daytime when turbulence was dominated by larger-scale eddies.

[18] Spectral analysis was used to further validate the observed fluxes. Average cospectra (Figure 4b) for $\langle w'T_s' \rangle$ and $\langle w'PAN' \rangle$ indicate that the majority of flux is transported by eddies in the range $f = 0.005-0.1$ (where f is the normalized frequency defined as nz/U, where n is the natural frequency and U is the wind speed). This is typical of transport over large forested canopies due to the large coherent eddy structures that dominant turbulent transport [*Amiro*, 1990; *Kaimal and Finnigan*, 1994]. For PAN, there is nearly no flux contribution at normalized frequencies greater than 0.35. It is unclear why there is loss at the high frequency end of the spectrum. Comparison with temperature cospectra suggest that PAN fluxes may be underestimated by ~19% on average. There is also considerable "white" noise in the power spectra of PAN in the high frequency region which adds to the overall uncertainty in the flux measurement [*Lenschow and Kristensen*, 1985] (discussed further in section 3.4). PPN and MPAN show similar tendencies in their spectra.

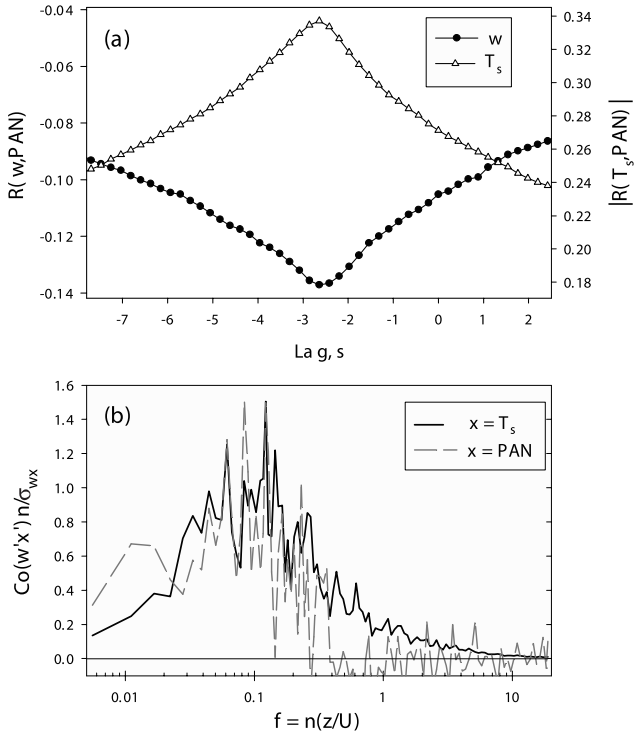

Figure 4. (a) Average cross correlation of w and T_s with PAN as a function of lag time. Data represents the average of all the 25-min. flux periods on July 19, 2003. The absolute value of the T_s cross correlation is shown (as the heat flux changes sign from day to night). Peaks correspond to the lag induced by the flow down the inlet line. (b) Cospectrum of $w'T'_s$ and w'[PAN]' for the same time periods as in Figure 4a. Spectra are multiplied by frequency and normalized by the total covariance.

[19] As with PAN, comparison of cospectra for $\langle w'T'_s\rangle$ and $\langle w'NO'_y\rangle$ indicated little flux contribution to the NO_y flux at normalized frequencies greater than 0.25, suggesting that NO_y fluxes were, on average, underestimated by ~20–25%. However, a more serious problem arises from the short glass inlet tube. Previous work has shown that gas phase HNO_3 is lost initially on glass, but that the surface becomes conditioned after a period of a few hours [*Neuman et al.*, 1999]. For this reason we tested the transmission of this type of inlet after the mission using a CIMS for detection of HNO_3 [*Huey et al.*, 1998]. These tests demonstrated that only 35–40% of the HNO_3 was transported immediately through the glass inlet. The surface conditioning noted by *Neuman et al.* [1999] may also not be applicable under the high humidity conditions encountered during this experiment. Although the loss of HNO_3 would not significantly impact the NO_y concentration measurements (as HNO_3 is typically only ~5–12% of the total NO_y [*Williams et al.*, 1997, 1998]), they would have a large impact on the measured fluxes. Therefore, this evidence, along with uncertainties about the conversion efficiency of HNO_3 within our converter, suggests that the NO_y fluxes presented here should be considered more of a lower limit.

[20] Deposition velocities were determined as $V_d = -F/\overline{\rho}_c$ where $\overline{\rho}_c$ is the mean density. For a species that is always deposited, the deposition velocity may be interpreted as the reciprocal of a total transfer resistance (R_t), which is composed of individual component resistances, reflecting physical constraints on the flux [*Wesely*, 1989; *Wesely and Hicks*, 2000]

$$R_t = 1/V_d(z-d) = R_a(z-d) + R_b + R_c. \quad (6)$$

Here R_a, the aerodynamic resistance to mass transfer, describes the turbulent transport and is defined by

$$R_a(z-d) = \frac{\overline{u}(z-d)}{u_*^2} - \frac{\Psi_H(\xi) - \Psi_M(\xi)}{ku_*} \quad (7)$$

where $\overline{u}(z-d)$ = mean wind speed at height (z − d), u_* = friction velocity (= $|\langle u'w'\rangle|^{0.5}$), k = von Karman's constant (=0.4), $\xi = (z-d)/L$ where L is the Obukhov length ($L = \overline{T}_s u_*^3/kg\langle w'T'_s\rangle$, g = gravitation acceleration). $\Psi_H(\xi)$ and $\Psi_M(\xi)$ are the integrated stability corrections functions for heat (H) and momentum (M), respectively [*Dyer*, 1974]. R_b is the resistance to mass transfer across the laminar sublayer near the surfaces and depends on turbulence and the properties of species of interest and is usually expressed as $R_b = (Bu_*)^{-1}$ where B is the sublayer Stanton number. For the current study, we have used the formulations for B following the equations provided by *Jensen and Hummelshoj* [1995, 1997]. Other formulations [*Hicks et al.*, 1987; *Meyers et al.*, 1989] had little effect on results as this was generally a small term compared to the total surface resistance (see below). Note that the sum of R_a and R_b (i.e. $R_c \sim 0$) determine the maximum possible deposition velocity (V_{max}) such that

$$1/V_{max}(z-d) = R_a(z-d) + R_b \quad (8)$$

[21] R_c is the total surface resistance and is obtained via difference between the reciprocal of the measured deposition velocity and the sum of R_a and R_b. For a compound that is deposited both through stomates and to exterior surfaces, R_c can be expressed as the reciprocal sum of parallel component resistances [*Wesely*, 1989]:

$$\frac{1}{R_c} = \frac{1}{R_{st}} + \frac{1}{R_{ns}} \quad (9)$$

where R_{st} is the stomatal resistance, R_{ns} represents non-stomatal processes. These include cuticular resistance, resistance to elements in the lower canopy (branches, bark, etc.) and resistance at the ground surface. In the present study it is likely that the cuticular resistance is the most important (smallest in magnitude) of these non-stomatal deposition processes, as resistance to the lower canopy and ground surface must include a significant aerodynamic transfer resistance [*Wesely*, 1989] for a tall fully-leafed canopy such as the one in the present study.

3. Results and Discussion

3.1. Concentrations of PAN-Species

[22] Figure 5a shows a time series of the measured 30-min. average concentrations of PAN, MPAN, PPN and NO_y. Associated meteorological data are shown in Figure 5d.

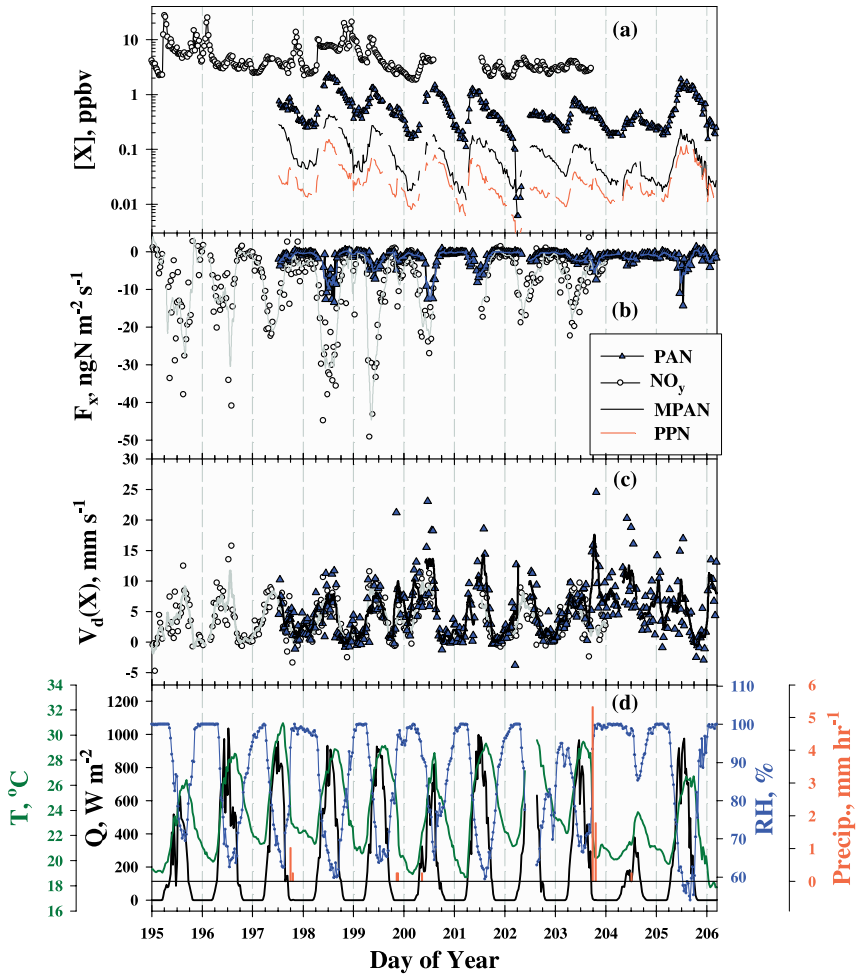

Figure 5. Time series of (a) PAN, PPN, MPAN and NO_y mixing ratio (b) mass fluxes of PAN and NO_y, (c) Deposition velocities of PAN and NOy and (d) meteorological variables (radiation, temperature, relative humidity and precipitation). The lines drawn in and Figures 5b and 5c are 5-point running means to the data points. Time reported is local standard time.

Average diurnal profiles of PAN and NO_y concentrations are given in Figure 6a. Concentrations of PAN species tended to peak during midday due to photochemical production and then experience a slow decay late in the day and continuing through the night. This afternoon decay is likely due to lower production rates and high thermal dissociation rates (higher temperatures and larger NO/NO_2 ratios), with deposition continuing to deplete PANs through the night. NO_y concentrations peak early in the morning most likely due to strong local sources and venting of the nocturnal boundary layer. As the boundary layer height and turbulent mixing increased, concentrations began to decay. High concentrations were again observed in the evening during the transition to the nocturnal boundary layer – most likely due to late afternoon traffic patterns and the collapsing of the daytime mixed boundary layer. There were also periodic "spikes" in NO_y concentration which were not accompanied by increases in [PAN]. They were, however, accompanied by sharp increases in NO_x measured above the canopy (Toohey, unpublished data). Thus, these appeared to be the influence of "fresh" local pollution sources advecting past the tower location. Daytime [PAN]/[NO_y] was 0.17 ± 0.06 (1σ), dropping to 0.10 ± 0.05 (1σ) at night. These ratios were accompanied by changes in the NO_x/NO_y ratio from 0.4–0.5 during daytime to 0.6–0.8 at night. These observations are quite similar to those reported in past studies of mildly polluted air masses [*Williams et al.*, 1997, 1998; *Roberts et al.*, 2002].

[23] Mass spectra (Figure 7) were taken daily both as a check on data quality and to assess the importance of other PAN type compounds. As demonstrated in Figure 7, PAN is by far the dominant species observed with PPN at about 6–8% of the PAN. MPAN signal levels were typically 2–3% of PAN values which corresponds to a relative mixing ratio of 16–24%. Again, these ratios are typical of previously measured ratios [*Roberts et al.*, 2002]. There are at least 10 other significant peaks in the mass spectra at signal levels corresponding to more than 20 pptv (assuming maximum sensitivity). Several of these peaks such as MoPAN (75 amu, $CH_3OC(O)O_2NO_2$), isomers of butyl peroxy nitrates (87 amu, $C_3H_7C(O)O_2NO_2$), and PBzN (121 amu, $C_6H_5C(O)O_2NO_2$) are tentatively assigned in the mass spectra based on previous work [*Slusher et al.*, 2004; Swanson et al., manuscript in preparation, 2006]. The mass

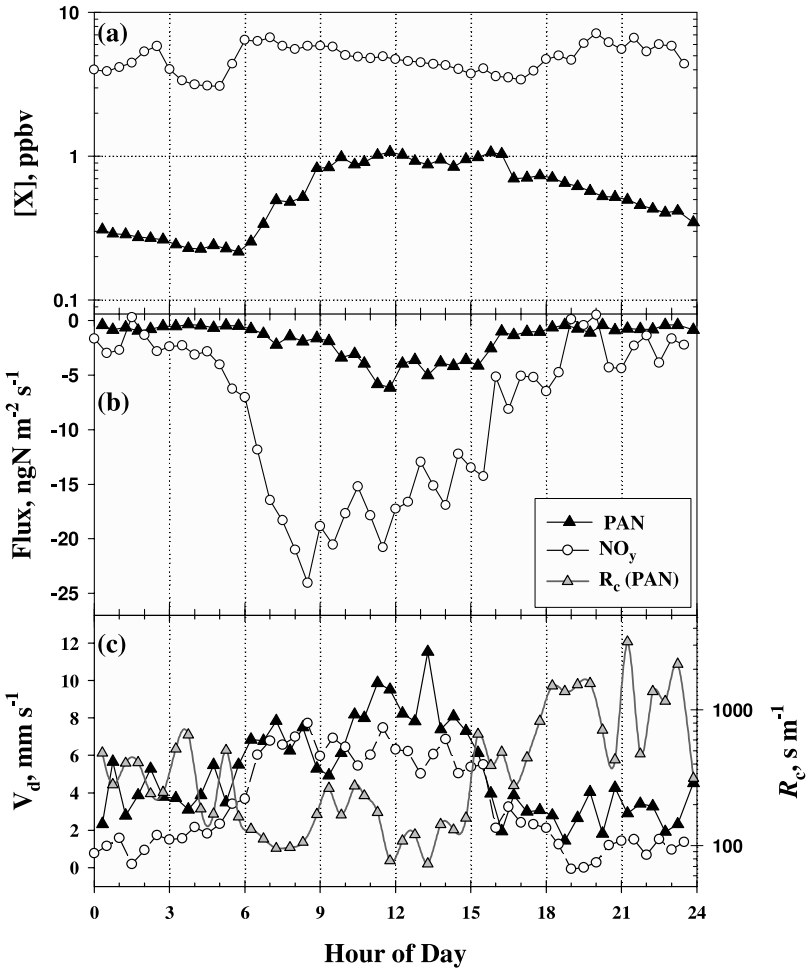

Figure 6. Diurnal average for PAN and NO_y of (a) mixing ratio (b) flux, (c) deposition velocity and surface resistance, R_c (for PAN only). Time reported is local standard time.

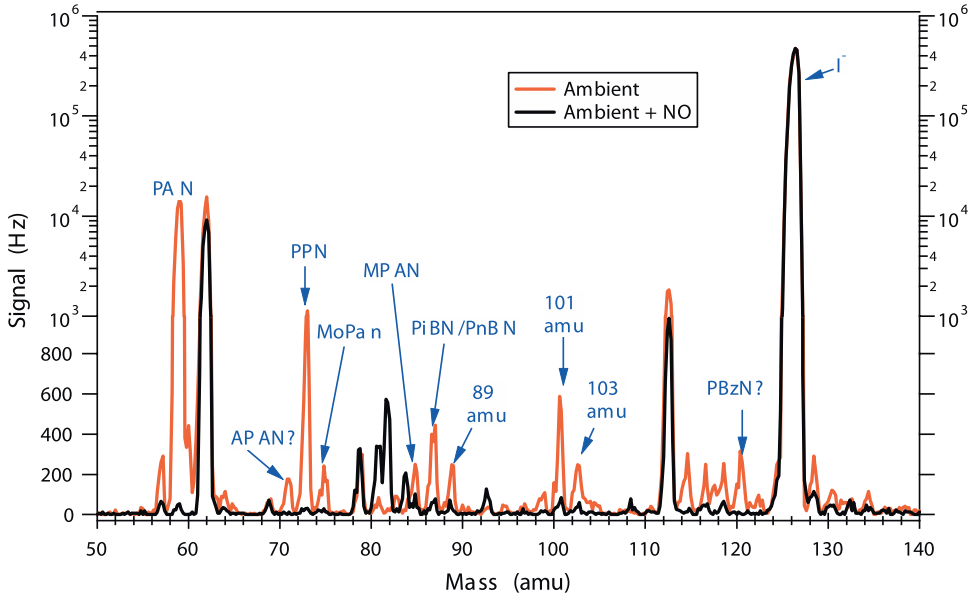

Figure 7. Typical mass spectrum from TD-CIMS instrument taken on the afternoon of July 18, 2003. The red line is the signal from an ambient measurement and the black line is signal during a background measurement, i.e. excess NO addition. The PAN signal is equivalent to a mixing ratio of 1.7 ppbv. Note that the y-axis is logarithmic above 1000 Hz and linear below.

peak that was consistently found to be the third most abundant and often nearly as intense as PPN was observed at 101 amu. This peak nominally corresponds to isomers of peroxy pentyl nitrates (i.e. $C_4H_9C(O)O^-$ from $C_4H_9C(O)O_2NO_2$) but we feel that this is unlikely as these products are expected to be smaller than the butyl peroxy nitrates. Another potential structure would be a four carbon hydroxylated PAN with one site of unsaturation (i.e. $HOC_3H_4CO_2^-$ from $HOC_3H_4C(O)O_2NO_2$). However, this structure is not expected in high yield from isoprene oxidation and at this time is unassigned. The peak at 89 amu was also often found to be larger than the butyl peroxy nitrates. This peak could correspond to a three carbon PAN compounds (i.e. a formula of $C_2H_5OCO_2^-$ possibly formed from $HOCH_2CH_2C(O)O_2NO_2$ or $CH_3CH_2OC(O)O_2NO_2$) and is also unassigned at this time. Consequently, future work on the identification of these two compounds is needed, in particular, because they may represent markers for oxidation of biogenic hydrocarbons such as isoprene.

3.2. Fluxes and Deposition Velocities

[24] Along with the concentration data in Figure 5, measured fluxes and deposition velocities for PAN are shown in Figures 5b and 5c. Fluxes and V_d of NO_y are also given to provide a sense of scale. Measured NO_y fluxes and deposition velocities were similar in magnitude to those reported by *Munger et al.* [1996] over a temperate deciduous forest. Average diurnal profiles of these quantities are given in Figure 6. Fluxes show a high degree of variability, but were consistently negative (deposition) for all PAN species as well as NO_y. The few small positive PAN fluxes were within the statistical uncertainty of zero or were the result of nonstationarity in the local turbulence. Fluxes of PPN and MPAN (not shown) consistently followed similar behavior to those of PAN. However, due to the lower signal to noise for these compounds, fluxes and deposition velocities showed higher variability (and larger uncertainties); therefore, much of our following analyses center primarily on PAN. We have omitted NO_y fluxes from periods where NO_y concentrations increased or decreased by more than 3 ppbv from the previous half hour. These conditions were due to influence of local pollution sources and led to highly variable NO_y fluxes. Since NO_y is a combination of different individual compounds, each of which has its own depositional characteristics, a large change in the NO_y partitioning during the flux-averaging period can induce large variability in the measured eddy flux.

[25] PAN, PPN and MPAN fluxes indicated diurnal profiles, which to some degree, mirrored diurnal concentration trends (Figure 8a). Average midday fluxes of PAN peaked at -6.0 ng N m^{-2} s^{-1} with individual flux measurements up to -14 ng N m^{-2} s^{-1} (Figure 5b) Ratios of the fluxes of PPN and MPAN to PAN were similar to the concentration ratios (F_{MPAN}/F_{PAN} = 0.22 ± 0.12 and F_{PPN}/F_{PAN} = 0.07 ± 0.03, errors = 1σ). The fluxes of MPAN and PPN peaked (on average) at -1.3 and -0.4 ng N m^{-2} s^{-1}, respectively, at midday. A diurnal pattern was still observed in the deposition velocity (Figures 6c and 8b) after normalization by concentration. All three PAN compounds exhibited similar diel profiles in deposition velocity (Figure 8b) although PPN and MPAN showed much larger variability. A small maximum was observed just after dawn,

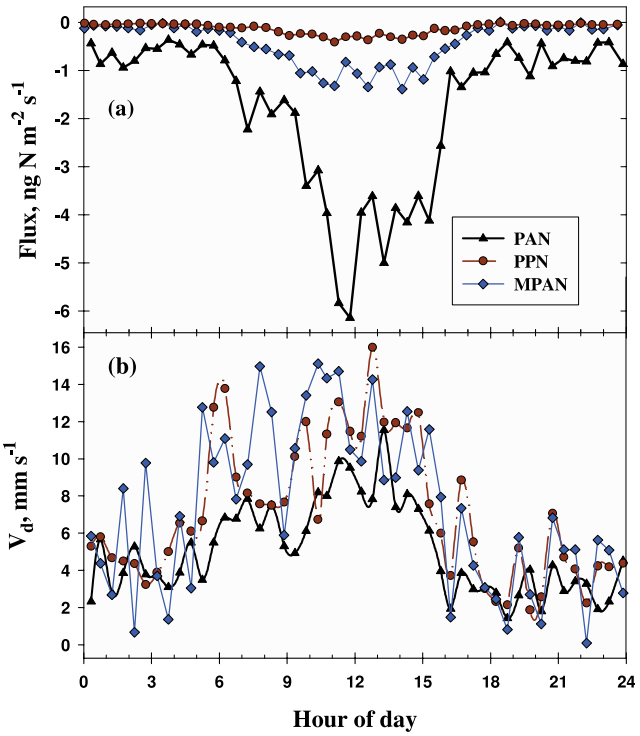

Figure 8. Diurnal average of (a) fluxes and (b) deposition velocities for PAN, PPN and MPAN.

followed by a larger midday maximum. NO_y deposition velocities also exhibited a diurnal trend with larger V_d during daytime periods. There was no indication of a compensation point for the PAN compounds, which would have been indicated by emission at low concentration. PAN deposition accounted for 20% of the total daytime NO_y uptake, and the typical midday flux ratio (F_{PAN}/F_{NOy}) was ~0.25–0.3 (Figure 6). Note that due to NO_y flux uncertainties discussed in section 2.3, these ratios are likely upper limits to PAN contribution to the NO_y flux.

3.3. Chemical Contributions to the Eddy Flux of PAN

[26] The complete mass balance equation for PAN is

$$F_z + \frac{\partial}{\partial t}\int_0^z C(z)dz = \int_0^z P(z)dz - \int_0^z L(z)dz - \int_0^z D(z)dz \quad (10)$$

where $P(z)$, $L(z)$ and $D(z)$ are the height-dependent chemical production, chemical loss, and deposition, respectively (where z is the measurement height for the turbulent flux). $c(z)$ is the PAN concentration, which integrated over height represents the storage of PAN below the eddy flux measurement height. During convectively well-mixed periods, this term is small and can be neglected. Furthermore, since PAN is not emitted or chemically produced at night, no buildup of PAN below the sensor height occurs and this storage again remains small.

[27] To understand the contributions of the chemical loss and production terms to the total flux, one must consider the time scales of these processes relative to that of turbulent transport. For a scalar to be chemically-conserved (i.e., for

the P and L terms to become relatively unimportant), its chemical lifetime must be significantly larger than that for transport. The time scale for transport can be determined from the integral turbulence time scale (τ_w), which is determined from the autocorrelation of the w-time series [*Kaimal and Finnigan*, 1994; *Lenschow*, 1995]. The integral time scale signifies the peak frequencies at which flux is transported over a given time period (i.e., the peak of the cospectrum). Daytime values during this study for τ_w were 20–30 s, typical of convective conditions over forested canopies [*Amiro*, 1990]. Nighttime values of τ_w increased upwards to 60–80 s.

[28] PANs are produced through the photochemical oxidation of hydrocarbons. Production is nearly zero at night and depends primarily on reactive hydrocarbon oxidation rates by OH radicals during the day. At the Duke site, measurements suggested that the primary PA precursor molecules at midday included acetaldehyde (1–2 ppbv), methacrolein and methyl vinyl ketone (sum of MACR and MVK was 2–4 ppbv) (Karl, personal communication). Assuming typical midday OH concentrations ([OH] $\sim 5 \times 10^6$ molec cm^{-3} [*Tanner et al.*, 1997]), typical lifetimes for these compounds were $\geq$1.6 hours, much longer than the time for vertical turbulent transport. It should also be noted that MACR is the only source of MPAN.

[29] Chemical loss of PAN is primarily via reactions (1f), followed by reaction (2). Thus its lifetime with respect to loss is dependent on the thermal decomposition of PAN and the NO/NO$_2$ ratio [*Orlando et al.*, 1992; *Shepson et al.*, 1992a]:

$$\tau_{PAN} = \frac{1}{k_{1r}}\left(1 + \frac{k_{1f}[NO_2]}{k_2[NO]}\right) \tag{11}$$

At night NO is titrated nearly completely to NO$_2$ by excess O$_3$ via reaction (4), thus the PAN lifetime becomes exceedingly long ($\tau_{PAN} > 6$ hours) and thermal loss becomes unimportant. During daytime periods, the experimentally-determined [NO$_2$]/[NO] and temperature-dependent rate coefficients were used to calculate loss lifetimes of $\tau_{PAN} \geq 1000$ s (16.7 min). Thus, the daytime ratio of τ_{PAN}/τ_w was $\geq$30 for both production and loss terms. Therefore it appears that chemical contributions to the observed turbulent fluxes were small and contained in the low frequency concentration trends over the flux period duration. *Doskey et al.* [2004] reached the same conclusion over a short grassland canopy using the flux-gradient method.

3.4. Error in the Flux Measurements

[30] A substantial degree of "white noise" was noted in the high frequency end of the power spectrum for both the PAN and NO$_y$ measurements. As described by *Lenschow and Kristensen* [1985], the presence of uncorrelated instrumental noise does not necessarily mean a loss of flux insomuch as an increase in the overall error of the flux measurement. The overall error in the fluxes (σ^2_{err}) can be described by [*Lenschow and Kristensen*, 1985; *Ritter et al.*, 1990]:

$$\sigma^2_{err}(F) \cong \frac{\sigma^2_w}{T}\left(4\sigma^2_c\tau_w + \sigma^2_n\Delta t\right) \tag{12}$$

where T is the averaging period (25 min.), Δt is the sampling time (=0.22 s) and the variances (denoted as σ^2) due to vertical velocity (w), true variability in concentration due to atmospheric fluctuations (c) and uncorrelated noise (n). The first term on the right hand side in equation 12 describes the random sampling error whereas the second term describes the contribution due to instrument noise. This equation can be rearranged to a form which estimates the relative error in the flux:

$$\frac{\sigma_{err}}{\langle w'c'\rangle} \cong \frac{1}{R_{wc}}\left[\frac{4\tau_w}{T} + \left(\frac{\sigma^2_{c,m}}{\sigma^2_c} - 1\right)\frac{\Delta t}{T}\right]^{1/2} \tag{13}$$

where R_{wc} is the correlation coefficient between w and c, and $\sigma^2_{c,m}$ is the total measured concentration variance:

$$\sigma^2_{c,m} = \sigma^2_c + \sigma^2_n. \tag{14}$$

The true concentration variability (σ^2_c, or "noise-free variance" [*Ritter et al.*, 1990]) was estimated by assuming similarity with temperature:

$$R_{wT} \sim R_{wc} = \langle w'c'\rangle/\sigma_w\sigma_c) \tag{15}$$

and that the deposition velocity was some fraction (initially 1/4) of the maximum allowable (V_{max}). It follows, that σ_c may be approximated by:

$$\sigma_c \sim (0.25V_{max}\overline{\rho}_c)/R_{wT}\sigma_w \tag{16}$$

R_{wT} was observed to vary between 0.2 and 0.5 for most daytime conditions, similar to that for a depositing species [*Lenschow*, 1995] and using this in equation (13) yielded typical relative flux error estimates for single flux measurements of ±41% and ranged between 25–65% for each 25 or 30 minute flux value.

3.5. Stomatal Contribution to PAN Uptake

[31] Deposition velocities for PAN indicated a midday maximum, suggesting a link to plant activity. After correction for R_a and R_b (equation (6)), R_c also showed lower resistance values during daytime (Figure 6c). This midday minimum is consistent with uptake through the stomates in support of the measurements of *Sparks et al.* [2003] and *Doskey et al.* [2004]. Minimum daytime resistance values were on the order of 70–130 s m^{-1}.

[32] The canopy-level stomatal resistance to PAN, R_{st}(PAN), was determined by first estimating the canopy resistance for H$_2$O, then correcting for differences in diffusion coefficients:

$$R_{st}(PAN) = \frac{D_{H2O}}{D_{PAN}}R_{st}(H_2O) \tag{17}$$

where D_i is the diffusion coefficient of either PAN (0.089 cm^2 s^{-1} [*Wesely*, 1989; *Sparks et al.*, 2003]) or water vapor (0.227 cm^2 s^{-1} [*Monteith and Unsworth*, 1990]). The canopy resistance for water vapor was estimated in two ways: (1) inversion of the Penman-Monteith equation [*Monteith and Unsworth*, 1990] and (2) calculation of the

water vapor gradient across the leaf (needle) boundary layer surfaces (as described by *Thom* [1975] and *Fowler et al.* [2001]). Both methods rely on input values of the canopy-level water vapor flux and assume that this flux originates solely from transpiration. Previous work at the Duke site suggests that, on a monthly average, the transpiration flux is 70–75% of the measured above-canopy total H_2O flux during the summer months [*Schäfer et al.*, 2002]. As this is averaged over nighttime and precipitation events, the typical daytime (non-precipitating conditions) ratio of E_{trans}/E_{total} (where E_{total} and E_{trans} are the total and transpiration water vapor fluxes, respectively) is likely to be between 0.8–0.9. We excluded periods early in the morning (when dew evaporation might be occurring) and when precipitation was measured. Assuming that 85% of the water vapor flux originates from transpiration, we find that both methods predict midday stomatal resistances for PAN of 200–250 s m^{-1}. Due to the parallel nature of the surface resistances (see equation (9)), it is more insightful to compare their reciprocals, i.e., the conductances ($g_{su} = 1/R_c$ and $g_{st} = 1/R_{st}$). The stomatal conductance (g_{st}) for PAN can then be directly compared with the total surface conductance to obtain the fraction of stomatal uptake. This plot is shown in Figure 9. The average $g_{st}/g_{su} = 0.45 \pm 0.03$ (error reported is the standard error, $\sigma/\sqrt{N}$, $N = 112$) from the inverted Penman-Monteith method and 0.48 ± 0.03 from leaf-boundary layer gradients. Although the data set is fairly small (due to gaps in the water vapor flux measurements), there appears to be no evidence for a limitation of stomatal transfer of PAN (i.e., $g_{su} \geq g_{st}$). It should be noted that a lower transpiration fraction would lead to a lower estimate of stomatal contribution (i.e., $E_{trans}/E_{total} = 0.7$, $g_{st}/g_{su} = 0.38$). An estimate of the stomatal uptake of PPN and MPAN will differ only by the ratio of diffusion coefficients relative to PAN. This work provides no information on the fate of the PAN that is deposited via stomatal uptake. The work of *Sparks et al.* [2003] observed that at least 80% of the nitrogen from PAN uptake remained in the leaf. Some NO_2 was emitted in their work, but it could not be definitely linked to PAN uptake [*Sparks et al.*, 2003]. In the current work, we can only assume that the nitrogen associated within PAN is assimilated within the plants.

[33] From these estimates of PAN stomatal resistance, it is clear that a large fraction of the observed PAN deposition is to other surfaces. From the current experiment, it is impossible to further partition the non-stomatal fluxes (resistances) to determine whether losses to soils, cuticles or tree boles and branches play significant roles. However, due to significant aerodynamic resistances to the ground surface and lower canopy elements within a forest canopy [*Wesely*, 1989; *Meyers et al.*, 1998], it is likely that PAN is primarily lost to plant cuticular surfaces. Future measurements of either PAN flux or concentrations within the canopy would help to further elucidate the sink distribution within the canopy.

3.6. Nighttime Fluxes and Surface Effects on PAN

[34] EC fluxes of both NO_y and the PAN-like compounds were lower at night, but remained significantly different from zero. It is interesting to note the sensitivity of the TD-CIMS is such that even at very low PAN concentrations (<200 pptv), significant correlations between [PAN] and vertical velocity were easily visible in the time series data (see Figure 2). Smaller fluxes were largely due to the reduced turbulent mixing in the nocturnal boundary layer (i.e., larger aerodynamic resistances, $R_a + R_b$). Although the strong nocturnal atmospheric stability tends to decouple airflows above and below the canopy, there still remains sheer-induced momentum transport to the upper canopy where deposition can occur. Thus the measured EC fluxes should represent depositional fluxes to the upper canopy [*Horii et al.*, 2004]. As seen in Figure 6c, typical nighttime deposition velocities ranged between 2–6 mm s^{-1}. The combination of low within-canopy transport and plant stomatal closure suggests that the primary loss pathway at night is via cuticular deposition in the upper canopy.

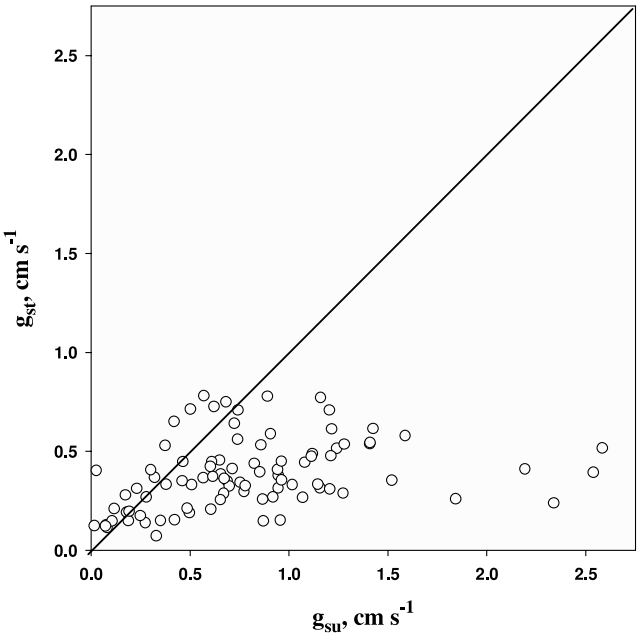

Figure 9. Plot of calculated canopy stomatal conductance for PAN (g_{st}) versus total surface conductance for PAN (g_{su}). The line drawn is the 1:1 line.

[35] At night, the photochemical pathways for production of PANs are absent. Also, since NO is primarily converted to NO_2 via reaction (4), chemical losses of PANs are also very slow ($\tau_{PAN} > 4$ hours). The studies of *Shepson et al.* [1992a, 1992b] were the first to exploit this nocturnal non-reactivity of PAN by observing nighttime concentration losses and relating them to deposition. Several other studies have since derived deposition rates using similar approaches [*Schrimpf et al.*, 1996; *McFadyen and Cape*, 1999a]. In the present study we also observed approximately exponential decreases in PAN concentration on four of the nights. Plots of $\ln[PAN]_t$ versus time were linear with slopes between $3.5–5.6 \times 10^{-5}$ s^{-1}. Following the simple boundary layer budget model presented by *Shepson et al.* [1992a], this slope, m, is related to the deposition velocity via, $m = -2V_d/h_{nbl}$ where h_{nbl} is the height of the nocturnal boundary layer height. Assuming a boundary layer height of 125 m on these nights leads to deposition velocities of 2.2–3.5 mm s^{-1}, in reasonable agreement with those derived by eddy covariance. Attempts to compare PAN deposition to that of ozone (similar to *Shepson et al.* [1992a]) were not successful as

decays of ozone were not exponential. This suggests that chemistry other than deposition was influencing its concentration, most likely involving NO_x chemistry (titration via reaction (3)). However, ozone always remained in excess over NO_x during the PAN study, so that nighttime chemical losses of PANs were minimized.

[36] Deposition velocities tended to be at a minimum (and R_c – a maximum) just after sunset. This was followed by a slow increase through the night (Figure 6c). This led to small, relatively constant depositional fluxes at decreasing PAN concentrations. These trends were mirrored in the deposition velocities of PPN and MPAN (Figure 8, although with larger scatter in the data). The large degree of variability in these V_d measurements originated from many sources: small measured fluxes, large measurement uncertainty and the large uncertainties involved in estimating $R_a + R_b$ in low turbulence conditions. However, it also appears that surface conditions play a key role in governing the deposition velocity, especially at night. Figure 10 shows plots of the measured deposition velocities (V_d(PAN)) versus the maximum deposition velocity allowable by turbulence (V_{max}) with different symbols noting different surface conditions (dry or wet). We have compared to V_{max} to remove differences caused by changes in turbulent transport. We had no direct measure of surface wetness available; therefore, we defined the surfaces to be wet either (1) during and immediately following precipitation events or (2) when relative humidity at 26 m was >96% (which would include dew formation). As can be seen in the figure, there is a significant increase in the deposition velocity during wet time periods. This implies a lowering of surface resistance to PAN uptake. Although most of the wet periods occur at night, Figure 10 includes daytime wet periods as well. On average, $V_d(PAN)/V_{max}$ = 0.23 ± 0.02 (standard error, N = 217 time periods) under dry conditions and 0.51 ± 0.03 (standard error, N = 158 time periods) under wet conditions. The median non-stomatal surface resistance, R_{ns}, decreased from 244 s m^{-1} under dry conditions to 125 s m^{-1} when surfaces were wet. Mean R_{ns} values were higher (650 s m^{-1} when dry, 300 s m^{-1} when wet) due to a small number of data points with high surface resistances (i.e., very small fluxes), but showed the same trend.

[37] Our definition of wetness is rather oversimplified, as layers of water on leaf surfaces have been observed at relative humidities >70% [*Burkhardt et al.*, 1999]. Nearly all time periods during this experiment had relative humidities (at z = 26 m) $\geq$ 70% (see Figure 5d), thus we must assume that a layer of water molecules always resided on the needle surfaces. However, as seen in Figure 10, there is clearly a significant change in deposition characteristics at very high relative humidity. Our designation of "wet" likely corresponds to cases where actual condensation or water drops would have been easily visible on needle surfaces. We also noted several periods where the ratio of $V_d(PAN)/V_{max}$ dramatically increased following precipitation events (on DOY 201, see Figures 5c and 5d). The ratio remained high until the combination of solar radiation and decreasing relative humidity suggested that the majority of water from leaf surfaces had evaporated. Wetness effects may also aid in describing the diurnal trends in the PAN deposition velocity (Figure 6c). The slow increase in V_d(PAN) through the nighttime hours may be explained by dew accumulation.

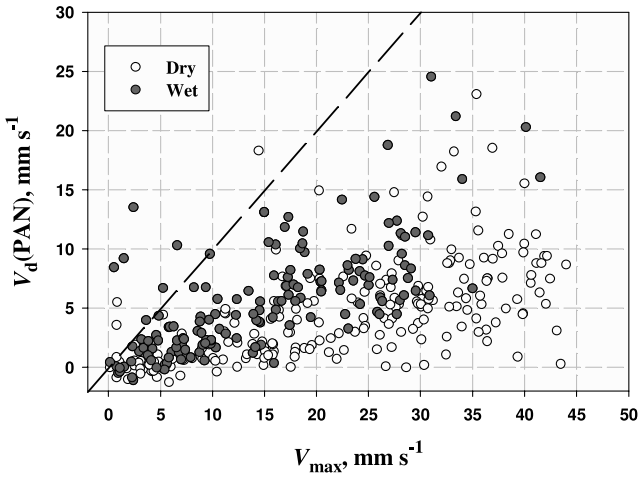

Figure 10. Plot of V_d(PAN) versus V_{max} indicating wet and dry periods. Line drawn is the 1:1 line.

We also observe a small maximum in V_d(PAN) just after sunrise (Figure 6c). This coincides with the breakdown of the nocturnal boundary layer and the transport of PAN from the residual layer above (where it is both thermally and chemically stable overnight) to the surface. Here it encounters wet surfaces as dew has not yet evaporated and the relative humidity remains near saturation. As surfaces dry out, deposition velocities decrease in mid-morning before increasing to a midday maximum due to stomatal uptake.

[38] These observations indicate a definite impact of leaf surface water on PAN deposition. This is rather unexpected based on the solubility of PAN in water at pH's typical of dew or precipitation. The effective Henry's law constant is 4.1 M atm^{-1} and its hydrolysis in pure water is slow (k = 3.9 × 10^{-4} s^{-1} at 293 K [*Kames and Schurath*, 1995]). Earlier work by *Kames et al.* [1991] obtained an estimate of the deposition velocity of PAN to water of only 0.08 mm s^{-1} which appeared limited by the hydrolysis rate. It has also been observed that PAN is not effectively scavenged by clouds [*McFadyen and Cape*, 1999b] and can be transported relatively large distances over oceans [*Jacobi et al.*, 1999], in accordance with the solubility and hydrolysis measurements. Based on this solubility, *Shepson et al.* [1992a] hypothesized that PAN deposition might be reduced with wet surfaces. *Schrimpf et al.* [1996] indicated no dependence of nocturnal PAN V_d with relative humidity, although inspection of their data (see Figure 4 in *Schrimpf et al.* [1996]) suggests that, if anything, PAN deposition velocities tended to increase with increasing relative humidity, not decrease. These authors do note that they excluded periods with dew formation, although no reason was given as to why.

[39] To explain our observations, it is necessary to have an uptake mechanism that operates at similar time scales to turbulent transport (~30–180 s at night). *Roberts et al.* [1996] suggested rapid scavenging of the PA radical by droplets to explain observed PAN losses during a fog event. However, this mechanism is limited by PAN thermal decomposition which is much slower than the turbulent transport at night. Therefore it appears that some form of uptake of PAN itself into the surface needle water is necessary to explain the observed PAN deposition.

[40] The chemical composition of leaf surface water during our study was not known and likely highly variable. It is known that there are numerous factors which can affect the composition and chemical reactivity of leaf/needle surface water. Plant exudate and guttation processes (both current and from previous days), codeposition (or prior deposition of species that are stable on the surface) of gases, dust, particles, etc., can all affect solution properties such as pH, chemical composition and reactivity [*Wesely et al.*, 1990; *Erisman and Wyers*, 1993]. *Wesely et al.* [1990] found that plant surfaces often tended to partially neutralize dew water relative to surrogate Teflon surfaces. However, pH values in their study (pH ranging from 4–6) were still well below values where PAN hydrolysis is efficient (pH > 7). Therefore, it seems more likely that there is some form of reactive uptake responsible for the observed deposition enhancement. Whether the origin of the species reacting with PAN is from the vegetation or from a codepositing species (e.g., NH_3) is unknown at this point. It is interesting to note that similar enhancement in O_3 deposition by surface wetness has been observed over forests [*Fuentes et al.*, 1992; *Lamaud et al.*, 2002; *Finkelstein et al.*, 2000], though O_3 is even less soluble than PAN (H_{O3} = 10^{-2} M atm^{-1} [*Wesely*, 1989]).

3.7. Comparisons to Past Work

[41] Work concerning PAN uptake has been scarce due to prior measurement difficulties. Early enclosure and wind tunnel studies suggested deposition velocities that were $\sim 0.5 V_d(O_3)$ [*Hill*, 1971; *Garland and Penkett*, 1976]. These studies reported values of 2.5 to 7.5 mm s^{-1} over grass or alfalfa, respectively. More recently, studies over short canopies (primarily grasses) reported quite low deposition velocities for PAN (V_d = 0.9–2.3 mm s^{-1}) [*Dollard et al.*, 1990; *Doskey et al.*, 2004]. *Doskey et al.* [2004] also estimated from a theoretical standpoint that uptake via diffusion into cuticular surfaces would be unimportant relative to stomatal uptake; however, they note that this does not account for reactions with possible biochemicals present. The importance of stomatal uptake has been demonstrated at the leaf level by *Sparks et al.* [2003] and *Teklemariam and Sparks* [2004].

[42] However, PAN deposition velocities derived over taller or forested canopies have typically been much larger. As noted in the previous section, *Shepson et al.* [1992a] used nocturnal losses of PAN and the boundary layer height to deduce a deposition velocity of 5.4 mm s^{-1}. They also noted that $V_d(PAN) \sim 2.4 V_d(O_3)$, in contrast to the earlier studies [*Shepson et al.*, 1992a]. *McFadyen and Cape* [1999a] also noted that nocturnal decays of PAN and O_3 suggested more rapid nighttime deposition of PAN. *Schrimpf et al.* [1996] measured nocturnal gradients of PAN relative to ^{222}Rn over corn to yield V_d(PAN) = 5.4 mm s^{-1}, in agreement with the Shepson et al. study. Since these studies were conducted at night when stomatal pathways were not operative, this suggests significant cuticular uptake (or uptake by other external plant surfaces), contrary to the theoretical postulates of *Doskey et al.* [2004]. *McFadyen and Cape* [1999a] postulated that daytime deposition fluxes of PAN could be much larger if stomatal uptake were included. Nighttime V_d(PAN) observed in this study by eddy covariance were in the range of 2–6 mm s^{-1}, in support of substantial cuticular deposition. Furthermore, our observation of enhanced PAN uptake during daytime suggests a significant stomatal component. It was estimated that ~45% of the total daytime deposition proceeded through plant stomates. Direct O_3 fluxes were not measured during the current work; however, past studies on O_3 deposition [*Munger et al.*, 1996] suggest nocturnal $V_d(O_3)$ of <2 mm s^{-1} over forests. Therefore our study supports the previous works suggesting $V_d(PAN) > V_d(O_3)$ at night.

[43] There have been no direct measurements on the effects of surface wetness on PAN deposition. The original studies of *Garland and Penkett* [1976] noted that wet soils tended to enhance PAN uptake, but the effect was fairly small (from 2 mm s^{-1} on dry soil to 3 mm s^{-1} on wet soil). The data of *Schrimpf et al.* [1996] suggest a dependence of V_d(PAN) on relative humidity, but due to variability in the data, no statistically significant relationship could be determined. Although little evidence for surface wetness effects exist regarding PAN deposition, it is interesting to note that contradictory evidence for other reactive species, notably O_3, has been reported. Both depositional enhancements [*Fuentes et al.*, 1992; *Lamaud et al.*, 2002; *Finkelstein et al.*, 2000] and reductions [*Wesely et al.*, 1978; *Hicks et al.*, 1987; *Grantz et al.*, 1997] of O_3 have been observed as a result of surface wetness. In fact, it appears that these wetness effects for ozone may be species-dependent [*Fuentes et al.*, 1994] as well as dependent on solution constituents. Further work is needed to see if similar behavior is observed for PAN uptake.

[44] To our knowledge, there have been no previous studies of the deposition of PPN and MPAN to surfaces. Thus, our work represents the first flux measurements for these compounds. Although the uncertainty in the PPN and MPAN measurements is greater than those of PAN, the similar patterns noted in the measured fluxes and deposition velocities suggest that these compounds undergo similar surface interactions as does PAN.

3.8. Implications and Application Toward Depositional Modeling of PAN

[45] As suggested by *Sparks et al.* [2003], deposition of PAN and PAN-like compounds represent a source of atmospheric nitrogen to ecosystems that has so far been ignored. This study has shown that up to 20% of the total NO_y flux may be explained by PAN uptake. Of that, only ~45% of the PAN is directly taken up through the plant stomates where it could be rapidly assimilated. Contributions of other PAN-like compounds will be smaller and likely scale with their concentration ratio with [PAN]. Furthermore, wet deposition likely contributes similar amounts of nitrogen as dry deposition [*Lovett*, 1992] and ammonia deposition may also be significant. Therefore, it appears that PAN is likely a minor contributor to total ecosystem nitrogen deposition.

[46] From an atmospheric standpoint, an enhanced depositional process likely impacts in the role of PAN as a transporter of reactive NO_x from polluted to remote areas by affecting its atmospheric lifetime. In well-mixed boundary layer, the lifetime of a species with respect to deposition can be determined from $\tau_{dep} = z_m/V_d$, where z_m is the boundary layer height. So in a 1 km boundary layer and V_d = 10 mm s^{-1}, yields a lifetime of ~28 hours. On typical midsummer days

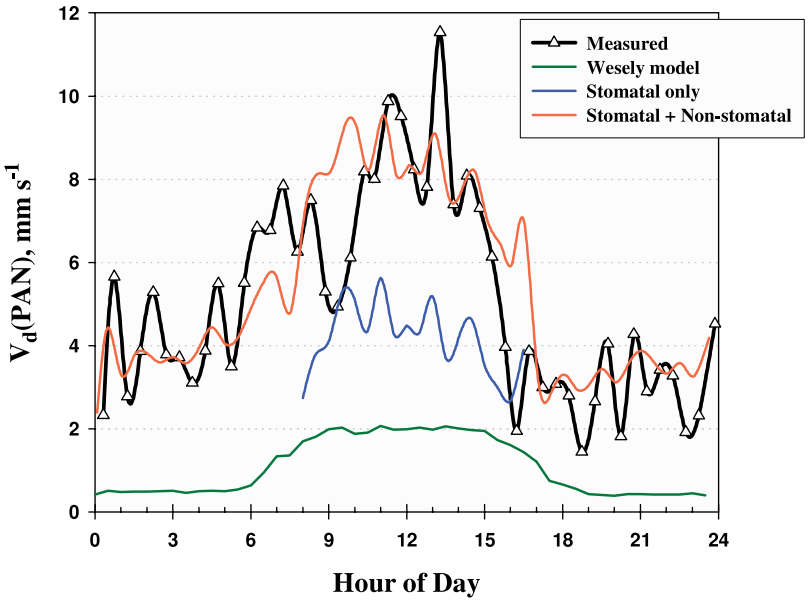

Figure 11. Plot of the measured diurnal profile of V_d(PAN) and those computed via the RADM model (green line) [*Wesely*, 1989], the stomatal contribution to PAN uptake as computed from the Penman-Monteith equation (blue line, assuming that transpiration equaled 85% of the measured water vapor flux), and combining the Penman-Monteith stomatal contribution with cuticular resistances of 125 s m^{-1} (wet) and 250 s m^{-1} (dry) (red line).

with NO/NO$_2$ ratios of ~0.2–0.5 and temperatures 25–35°C, the lifetime of PAN with respect to thermal decomposition and further reaction with NO is ~12–90 min. Thus, deposition cannot compete as a loss mechanism during these periods. However, at night, typical chemical lifetimes are often >6 hours, and the shallow boundary layer height further reduces the timescale for deposition. As a consequence, deposition becomes an important mechanism for depleting the nocturnal boundary layer of PAN and PAN compounds.

[47] Integrating over the entire diel cycle, the total PAN sinks due to deposition and thermochemical decomposition can be estimated via:

$$L_{dep} = \int_{24hr} [PAN] V_d dt \tag{18}$$

$$L_{chem} = \int_{24hr} [PAN] k' h_{bl} dt \tag{19}$$

[*McFadyen and Cape*, 1999a], where $k' = 1/\tau_{pan}$ and h_{bl} is the height of the boundary layer. We assume that the boundary layer height is approximately 125 m at night and 1 km during the day. During this study, deposition accounted for less than 3% of the PAN sink relative to thermochemical losses. This calculation overestimates the thermochemical loss, as surface temperatures were used to calculate the PAN lifetime for the entire boundary layer. However, even accounting for the lower temperatures with increasing altitude, it is unlikely that deposition can contribute more than 10% to the total daily PAN sink during the current study. This contrasts the findings of *McFadyen and Cape* [1999a], who suggested nearly equal losses via the two processes. However, their calculated chemical loss rate coefficients (k' in equation (19)) peaked midday between 8 and 25 × 10^{-6} s^{-1} (see Figure 7 in *McFadyen and Cape* [1999a]). This implies a PAN lifetime toward thermal degradation (and subsequent NO reaction) of greater than 10 hours. At typical daytime NO/NO$_2$ (~0.4), this requires temperatures of ~10°C or less. At these colder temperatures and assuming that V_d(PAN) is temperature independent, deposition would be capable of contributing nearly equally to the daily PAN sink. Therefore, it is likely that PAN deposition may be of greater importance in winter or in ecosystems at higher latitudes.

[48] Our findings here report the first direct measure of eddy covariance fluxes to a forest ecosystem and suggest that current models underestimate the deposition of PAN. In any depositional resistance model, basic assumptions have to be made concerning resistances to mass transfer at many key transfer points such as: plant cuticles, stomates, boles, branches, and soil surfaces. Concerning depositing species for which there is little or no prior experimental evidence, these assumptions are often based on either physical properties (solubility and hydrolysis) or comparisons to O$_3$ or SO$_2$ deposition (where there is considerable more experimental evidence) [*Wesely*, 1989; *Wesely and Hicks*, 2000]. For PAN, low solubility, slow hydrolysis and the early findings that V_d(PAN)/V_d(O$_3$) ~ 0.5, led the model parameterizations to predict the low deposition velocities shown in Figure 11. The widely-used RADM [*Wesely*, 1989] model predicts only significant stomatal uptake of PAN with midday deposition velocities for PAN of only ~2 mm s^{-1}. On average, we obtained daytime deposition velocities that are approximately a factor of 4–5 larger (~9.0–10.0 mm s^{-1}). We also note that canopy conductances calculated in the Wesely model were about a factor of two

lower than those estimated using either the Penman-Monteith equation or by boundary layer gradients of water vapor, thereby leading to lower estimates of PAN stomatal uptake (Figure 11).

[49] At night, the discrepancy is even larger, as our measured V_d(PAN) are often nearly an order of magnitude larger than the RADM model (4 mm s^{-1} measured to $\sim$0.5 mm s^{-1} in the model). The model has nearly no nighttime loss processes (typically $R_{ns} > 1300$ s m^{-1}) due to the low solubility of PAN and the assumed non-reactivity of PAN toward cuticular and the exterior surfaces of plants. With the growing evidence of nighttime depletion of PAN [*Shepson et al.*, 1992a, 1992b; *McFadyen and Cape*, 1999a] and the current direct flux measurements, these assumptions appear to be erroneous. Our results suggest non-stomatal (which we assume to be primarily cuticular) resistances of $\sim$250 s m^{-1} on dry surfaces, further decreasing to 125 s m^{-1} when plant surfaces were wet. However, the exact mechanism of this enhancement bears further study and it is not clear whether this phenomenon is characteristic of the leaf water layer chemistry for certain forest canopies or is ubiquitous. Combining these mean non-stomatal resistances (input as cuticular resistances) with estimates of stomatal uptake predicted from the Penman-Monteith equation, the model reproduces the basic shape and magnitude of the average diurnal deposition velocity (Figure 11). However, certain aspects of the diurnal profile, such as the early morning maximum, are not apparent in the model and bear further investigation.

[50] The underestimation of PAN deposition may be at least partially responsible for the tendency of global models to overestimate PAN concentrations systematically [e.g., *Horowitz et al.*, 2003; *von Kuhlmann et al.*, 2003; *Park et al.*, 2004]. Often these biases are as much as a factor of 2–3. The modeled PAN concentrations have been shown to be sensitive to (1) thermal decomposition rates, (2) source strength of isoprene, (3) upper tropospheric NO_x and (4) deposition of soluble intermediates in isoprene oxidation [*von Kuhlmann et al.*, 2003, 2004]; however, direct deposition of PAN itself has not been investigated. Although direct PAN deposition may not fully explain these observed discrepancies, it may be significant for some. For example, *von Kuhlmann et al.* [2003] report that their model overestimated the northern hemispheric surface PAN buildup during winter/spring. This would likely be a period during which PAN deposition could play a major role relative to thermal decomposition.

4. Conclusions

[51] We have successfully made the first eddy covariance measurements of peroxyacetyl nitrate (PAN), peroxypropionyl nitrate (PPN) and peroxymethacryloyl nitrate (MPAN) using the TD-CIMS thermal dissociation (TD-CIMS) technique. These studies demonstrate that PAN deposition proceeds much more efficiently than previously believed, at least over forested ecosystems. Deposition velocities for PAN were a factor of 4–5 greater than traditional deposition models would currently predict. Patterns in the deposition velocities of PPN and MPAN mirrored that of PAN. Although not competitive with thermal loss during the current study (due to warm temperatures), PAN deposition is likely to play a key role in the depletion of PAN in nocturnal boundary layers, and may become a major PAN loss mechanism at high latitudes or during colder season when thermal dissociation is slow. We also observed enhanced deposition when plant surfaces were wet, which is inconsistent with the low solubility of PAN. It is unclear as to the mechanism of this enhancement, but is likely due to residues dissolved in the surface needle water or possibly codeposition processes which can impact solution properties (pH and reactivity). This enhancement under wet conditions could be of great importance in places such as the tropics where PAN is a significant component of the atmospheric nitrogen budget due to the high emission of biogenic VOCs [*Singh et al.*, 1990]. Further study is needed to clarify the exact mechanism in order to determine whether the results here apply only to certain locations/ecosystems or can be applied universally.

[52] Furthermore, deposition mechanisms for PAN have only recently been investigated and information in this area remains rather cursory. The TD-CIMS technique has the potential to be instructive in many of these questions concerning PAN interactions with surfaces and, more specifically, plant canopies. The fast time resolution and high sensitivity of the TD-CIMS make it a valuable tool which be used in (1) leaf-level mechanistic studies, (2) canopy level profiling to determine sources and sinks within canopies [*Karl et al.*, 2004] and (3) ecosystem level eddy covariance fluxes (as shown in this study).

[53] **Acknowledgments.** The authors would like to thank the Duke FACE site and its staff for allowing us to work at their research site as well as the invaluable assistance they provided during this experiment. We would also like to thank Gabriel Katul and Paul Stoy for their assistance and permission to use data from the Duke Forest AmeriFlux data archives. NO, NO_x and O_3 data were provided by Darin Toohey and Linnea Avallone, and Alice Delia. The authors also would like to thank James Roberts of the NOAA Aeronomy Laboratory and Donald Lenschow, Thomas Karl and John Orlando of NCAR for their insight and suggestions. Andrew Turnipseed, Alex Guenther and Eiko Nemitz were funded via an interagency agreement with the USEPA National Risk Management Research Laboratory and would like to thank Chris Geron for his role as project manager and his assistance during this project. L. G. Huey and coworkers from the Georgia Institute of Technology were supported by NSF grant ATM-0115656. The Duke Forest site was supported by the Office of Science (BER), U.S. Department of Energy, grant DE-FG02-95ER62083.

References

Amiro, B. D. (1990), Comparison of turbulence statistics within three boreal forest canopies, *Boundary Layer Meteorol.*, *51*, 99–121.

Bridier, I., F. Caralp, H. Loirat, R. Lesclaux, B. Veyret, K. H. Becker, A. Reimer, and F. Zabel (1991), Kinetic and theoretical studies of the reactions $CH_3C(O)O_2 + NO_2 + M = CH_3C(O)O_2NO_2 + M$ between 248 and 393 K and between 30 and 760 torr, *J. Phys. Chem.*, *95*(9), 3594–3600.

Burkhardt, J., H. Kaiser, H. Goldbach, and L. Kappen (1999), Measurements of electrical leaf surface conductance reveal recondensation of transpired water vapour on leaf surfaces, *J. Plant Cell Environ.*, *22*, 189–196.

Cellier, P., and Y. Brunet (1992), Flux-gradient relationships above tall plant canopies, *Agric. For. Meteorol.*, *58*, 93–117.

Cox, R. A., and M. J. Roffey (1977), Thermal decomposition of peroxyacetylnitrate in the presence of nitric oxide, *Environ. Sci. Technol.*, *11*(9), 900–906.

Dollard, G. J., B. M. R. Jones, and T. J. Davies (1990), Dry deposition of HNO_3 and PAN, *A. E. R. E. Rep. R13780*, Harwell Lab., Oxfordshire, UK.

Doskey, P. V., Y. Fukui, D. R. Cook, and M. L. Wesely (2000), Measurements of the dry deposition of PAN above grass, in *Proceedings of the Symposium on Atmospheric Chemistry Issues in the 21st Century*, pp. 33–36, Am. Meteorol. Soc., Boston, Mass.

Doskey, P. V., V. R. Kotamarthi, Y. Fukui, D. R. Cook, F. W. Breitbeil III, and M. L. Wesely (2004), Air-surface exchange of peroxyacetyl nitrate at

a grassland site, *J. Geophys. Res.*, *109*, D10310, doi:10.1029/2004JD004533.
Dyer, A. J. (1974), A review of flux-profile relations, *Boundary Layer Meteorol.*, *7*, 363–372.
Erisman, J. W., and G. P. Wyers (1993), Continuous measurements of surface exchange of SO_2 and NH_3: Implications for their possible interaction in the deposition process, *Atmos. Environ.*, *27A*(13), 1937–1949.
Finkelstein, P. L., T. G. Ellestad, J. F. Clarke, T. P. Meyers, D. B. Schwede, E. O. Hebert, and J. A. Neal (2000), Ozone and sulfur dioxide dry deposition to forests: Observations and model evaluation, *J. Geophys. Res.*, *105*(D12), 15,365–15,377.
Fowler, D., C. Flechard, J. N. Cape, R. L. Storeton-West, and M. Coyle (2001), Measurements of ozone deposition to vegetation: Quantifying the flux, the stomatal and non-stomatal components, *Water Air Soil Pollut.*, *130*, 63–74.
Fuentes, J. D., T. J. Gillespie, G. Den Hartog, and H. H. Neumann (1992), Ozone deposition onto a deciduous forest during dry and wet conditions, *Agric. For. Meteorol.*, *62*, 1–18.
Fuentes, J. D., T. J. Gillespie, and N. J. Bunce (1994), Effects of foliage wetness on the dry deposition of ozone onto Red Maple and Poplar leaves, *Water Air Soil Pollut.*, *74*, 189–210.
Garland, J. A., and S. A. Penkett (1976), Absorption of peroxy acetyl nitrate and ozone by natural surfaces, *Atmos. Environ.*, *10*, 1127–1131.
Grantz, D. A., X. J. Zhang, J. W. Massman, A. Delany, and J. R. Pederson (1997), Ozone deposition to a cotton (Gossypium hirsutum L.) field: Stomatal and surface wetness effects during the California ozone deposition experiment, *Agric. For. Meteorol.*, *85*, 19–31.
Hicks, B. B., D. D. Baldocchi, T. P. Meyers, R. P. Hosker, and D. R. Matt (1987), A preliminary multiple resistance routine for deriving dry deposition velocities from measured quantities, *Water Air Soil Pollut.*, *36*, 311–330.
Hill, A. C. (1971), Vegetation: A sink for atmospheric pollutants, *J. Air Pollut. Control Assoc.*, *21*, 341–346.
Horii, C. V., J. W. Munger, S. C. Wofsy, M. Zahniser, D. Nelson, and J. B. McManus (2004), Fluxes of nitrogen oxides over a temperate deciduous forest, *J. Geophys. Res.*, *109*, D08305, doi:10.1029/2003JD004326.
Horowitz, L. W., et al. (2003), A global simulation of tropospheric ozone and related tracers: Description and evaluation of MOZART, version 2, *J. Geophys. Res.*, *108*(D24), 4784, doi:10.1029/2002JD002853.
Huey, L. G., E. J. Dunlea, E. R. Lovejoy, D. R. Hanson, R. B. Norton, and F. C. Fehsenfeld (1998), A chemical ionization mass spectrometer for fast time response measurements of HNO_3 in air, *J. Geophys. Res.*, *103*, 3355.
Jacobi, H.-W., R. Weller, T. Bluszcz, and O. Schrems (1999), Latitudinal distribution of peroxyacetyl nitrate (PAN) over the Atlantic Ocean, *J. Geophys. Res.*, *104*(D21), 26,901–26,912.
Jensen, N. O., and P. Hummelshoj (1995), Derivation of canopy resistance for water vapor over a spruce forest, using a new technique for the viscous sublayer resistance, *Agric. For. Meteorol.*, *73*, 339–352.
Jensen, N. O., and P. Hummelshoj (1997), Erratum to "Derivation of canopy resistance for water vapor over a spruce forest, using a new technique for the viscous sublayer resistance," *Agric. For. Meteorol.*, *85*, 289.
Kaimal, J. C., and J. J. Finnigan (1994), *Atmospheric Boundary Layer Flows: Their Structure and Measurement*, Oxford Univ. Press, New York.
Kames, J., and U. Schurath (1995), Henry's law and hydrolysis-rate constants for peroxyacetyl nitrates (PANs) using a homogenous gas-phase source, *J. Atmos. Chem.*, *21*, 151–164.
Kames, J., S. Schweighoefer, and U. Schurath (1991), Henry's law constant and hydrolysis of peroxyacetyl nitrate (PAN), *J. Atmos. Chem.*, *12*, 169–180.
Karl, T., M. Potosnak, A. Guenther, D. Clark, J. Walker, J. D. Herrick, and C. Geron (2004), Exchange processes of volatile organic compounds above a tropical rain forest: Implications for modeling tropospheric chemistry above a dense forest, *J. Geophys. Res.*, *109*, D18306, doi:10.1029/2004JD004738.
Katul, G. G., et al. (1999), Spatial variability of turbulent fluxes in the roughness sublayer of an even-aged pine forest, *Boundary Layer Meteorol.*, *93*, 1–28.
Lamaud, E., A. Carrara, Y. Brunet, A. Lopez, and A. Druilhet (2002), Ozone fluxes above and within a pine forest canopy in dry and wet conditions, *Atmos. Environ.*, *36*, 77–88.
Lenschow, D. H. (1995), Micrometeorological techniques for measuring biosphere-atmosphere trace gas exchange, in *Biogenic Trace Gases: Measuring Emissions From Soil and Water*, edited by P. A. Matson and R. C. Harris, pp. 126–163, Blackwell Sci., Malden, Mass.
Lenschow, D. H., and L. Kristensen (1985), Uncorrelated noise in turbulence measurements, *J. Oceanic Atmos. Technol.*, *2*, 68–81.
Lenschow, D. H., and M. R. Raupach (1991), The attenuation of fluctuations in scalar concentrations through sampling tubes, *J. Geophys. Res.*, *96*, 5259–5268.
Lovett, G. M. (1992), Atmospheric deposition and canopy interactions of nitrogen, in *Atmospheric Deposition and Forest Nutrient Cycling*, edited by D. Johnson and S. Lindberg, pp. 152–166, Springer, New York.
McFadyen, G. G., and J. N. Cape (1999a), Physical and chemical influences on PAN concentration at a rural site, *Atmos. Environ.*, *33*(18), 2929–2940.
McFadyen, G. G., and J. N. Cape (1999b), Springtime sources and sinks of peroxyacetyl nitrate in the UK and its contribution to acidification and nitrification of cloud water, *Atmos. Res.*, *50*, 359–371.
Meyers, T. P., B. J. Hueber, and B. B. Hicks (1989), HNO_3 deposition to a deciduous forest, *Boundary Layer Meteorol.*, *49*, 395–410.
Meyers, T. P., P. Finkelstein, J. Clarke, T. G. Ellestad, and P. F. Sims (1998), A multilayer model for inferring dry deposition using standard meteorological measurements, *J. Geophys. Res.*, *103*(D17), 22,645–22,661.
Monteith, J. L., and M. H. Unsworth (1990), *Principles of Environmental Physics*, 2nd ed., Edward Arnold, London.
Moxim, W. J., H. Levy II, and P. S. Kasibhatla (1996), Simulated global tropospheric PAN: Its transport and impact on NO_x, *J. Geophys. Res.*, *101*(D7), 12,621–12,638.
Munger, J. W., S. C. Wofsy, P. S. Bakwin, S. M. Fan, M. L. Goulden, B. C. Baube, A. H. Goldstein, K. E. Moore, and D. R. Fitzjarrald (1996), Atmospheric deposition of reactive nitrogen oxides and ozone in a temperate deciduous forest and a subarctic woodland: 1. Measurements and mechanisms, *J. Geophys. Res.*, *101*, 12,639–12,657.
Neuman, J. A., L. G. Huey, T. B. Ryerson, and D. W. Fahey (1999), Study of inlet materials for sampling atmospheric nitric acid, *Environ. Sci. Technol.*, *33*, 1133–1136.
Orlando, J. J., G. S. Tyndall, and J. G. Calvert (1992), Thermal-decomposition pathways for peroxyacetyl nitrate (PAN) – Implications for atmospheric methyl nitrate levels, *Atmos. Environ., Part A*, *26*, 3111–3118.
Park, R. J., K. E. Pickering, D. J. Allen, G. L. Stenchikov, and M. S. Fox-Rabinovitz (2004), Global simulation of tropospheric ozone using the University of Maryland Chemical Transport Model (UMD-CTM): 1. Model description and evaluation, *J. Geophys. Res.*, *109*, D09301, doi:10.1029/2003JD004266.
Ritter, J. A., D. H. Lenschow, J. D. W. Barrick, G. L. Gregory, G. W. Sachse, G. F. Hill, and M. A. Woerner (1990), Airborne flux measurements and budget estimates of trace species over the Amazon Basin during the GTE/ABLE-2B Expedition, *J. Geophys. Res.*, *95*(D10), 16,875–16,886.
Roberts, J. M., and S. B. Bertman (1992), Measurement of the thermal decomposition of peroxyacetic nitric anhydride (PAN) and peroxymethacrylic nitric anhydride (MPAN), *Int. J. Chem. Kinet.*, *24*, 297–307.
Roberts, J. M., et al. (1996), Episodic removal of NO_y species from the marine boundary layer over the North Atlantic, *J. Geophys. Res.*, *101*(D22), 28,947–28,960.
Roberts, J. M., F. Flocke, C. A. Stroud, D. Hereid, E. Williams, F. Fehsenfeld, W. Brune, M. Martinez, and H. Harder (2002), Ground-based measurements of peroxycarboxylic nitric anhydrides (PANs) during the 1999 Southern Oxidants Study Nashville Intensive, *J. Geophys. Res.*, *107*(D21), 4554, doi:10.1029/2001JD000947.
Schäfer, K. V. R., R. Oren, C. Lai, and G. G. Katul (2002), Hydrologic balance in an intact temperature forest ecosystem under ambient and elevated atmospheric CO_2 concentration, *Global Change Biol.*, *8*, 895–911.
Schrimpf, W., K. Lienaerts, K. P. Muller, J. Rudolph, R. Neubert, W. Schubler, and I. Levin (1996), Dry deposition of peroxyacetyl nitrate (PAN): Determination of its deposition velocity at night from measurements of the atmospheric PAN and 222Radon concentration gradient, *Geophys. Res. Lett.*, *23*, 3599–3602.
Shepson, P. B., J. W. Bottenheim, D. R. Hastie, and A. Venkatram (1992a), Determination of the relative ozone and PAN deposition velocities at night, *Geophys. Res. Lett.*, *19*, 1121–1124.
Shepson, P. B., D. R. Hastie, K. W. So, H. I. Schiff, and P. Wong (1992b), Relationships between PAN, PPN and O_3 at urban and rural sites in Ontario, *Atmos. Environ.*, *26A*, 1259–1270.
Simpson, I. J., G. W. Thurtell, H. H. Neumann, G. Den Hartog, and G. C. Edwards (1998), The validity of similarity theory in the roughness sublayer above forests, *Boundary Layer Meteorol.*, *87*, 69–99.
Singh, H. B., and P. L. Hanst (1981), Peroxyacetyl nitrate (PAN) in the unpolluted atmosphere: An important reservoir for nitrogen oxides, *Geophys. Res. Lett.*, *8*(8), 941–944.
Singh, H. B., D. Herlth, D. O'Hara, L. Salas, A. L. Torres, G. L. Gregory, G. W. Sachse, and J. F. Kasting (1990), Atmospheric peroxyacetyl nitrate measurements over the Brazilian Amazon basin during the wet season: Relationships with nitrogen oxides and ozone, *J. Geophys. Res.*, *95*(D10), 16,945–16,954.
Slusher, D. L., L. G. Huey, D. J. Tanner, F. M. Flocke, and J. M. Roberts (2004), A thermal dissociation-chemical ionization mass spectrometry

(TD-CIMS) technique for the simultaneous measurement of peroxyacyl nitrates and dinitrogen pentoxide, *J. Geophys. Res.*, *109*, D19315, doi:10.1029/2004JD004670.

Sparks, J. P., J. M. Roberts, and R. K. Monson (2003), The uptake of gaseous organic nitrogen by leaves: A significant global nitrogen transfer process, *Geophys. Res. Lett.*, *30*(23), 2189, doi:10.1029/2003GL018578.

Tanner, D. J., A. Jefferson, and F. L. Eisele (1997), Selected ion chemical ionization mass spectrometric measurement of OH, *J. Geophys. Res.*, *102*(D5), 6415–6425.

Teklemariam, T. A., and J. P. Sparks (2004), Gaseous fluxes of peroxyacetyl nitrate (PAN) into plant leaves, *Plant Cell Environ.*, *27*, 1149–1158.

Thom, A. S. (1975), Momentum, mass and heat exchange of plant communities, in *Vegetation and Atmosphere*, edited by J. L. Monteith, pp. 57–109, Elsevier, New York.

von Kuhlmann, R., M. G. Lawrence, P. J. Crutzen, and P. J. Rasch (2003), A model for studies of tropospheric ozone and nonmethane hydrocarbons: Model evaluation of ozone-related species, *J. Geophys. Res.*, *108*(D23), 4729, doi:10.1029/2002JD003348.

von Kuhlmann, R., M. G. Lawrence, U. Pöschle, and P. J. Crutzen (2004), Sensitivities in global scale modeling of isoprene, *Atmos. Chem. Phys.*, *4*, 1–17.

Warneck, P., and T. Zerbach (1992), Synthesis of peroxyacetyl nitrate in air by acetone photolysis, *Environ. Sci. Technol.*, *26*(1), 74–79.

Webb, E. K., G. I. Pearman, and R. Leuning (1980), Correction of flux measurements for density effects due to heat and water vapor transfer, *Q. J. R. Meteorol. Soc.*, *106*, 85–100.

Wesely, M. L. (1989), Parameterization of surface resistances to gaseous dry deposition in regional-scale numerical models, *Atmos. Environ.*, *23*, 1293–1304.

Wesely, M. L., and B. B. Hicks (2000), A review of the current status of knowledge on dry deposition, *Atmos. Environ.*, *34*, 2261–2282.

Wesely, M. L., J. A. Eastman, D. R. Cook, and B. B. Hicks (1978), Day-time variations of ozone eddy fluxes to maize, *Boundary Layer Meteorol.*, *15*, 361–373.

Wesely, M. L., D. L. Sisterson, and J. D. Jastrow (1990), Observations of the chemical properties of dew on vegetation that affect the dry deposition of SO_2, *J. Geophys. Res.*, *95*(D6), 7501–7514.

Williams, E. J., J. M. Roberts, K. Baumann, S. B. Bertman, S. Buhr, R. B. Norton, and F. C. Fehsenfeld (1997), Variations in NO_y composition at Idaho Hill, Colorado, *J. Geophys. Res.*, *102*, 6297–6314.

Williams, E. J., et al. (1998), Intercomparison of ground-based NO_y measurement techniques, *J. Geophys. Res.*, *103*(D17), 22,261–22,280.

F. Flocke, A. Guenther, and A. A. Turnipseed, Atmospheric Chemistry Division, National Center for Atmospheric Research, 1805 Table Mesa Dr., Boulder, CO 80307, USA. (turnip@ucar.edu)

J. Higgs, L. G. Huey, R. Stickel, and D. J. Tanner, School of Earth and Atmospheric Sciences, Georgia Institute of Technology, Atlanta, GA 30332, USA.

E. Nemitz, Centre for Ecology and Hydrology (CEH), Bush Estate, Penicuik, Midlothian EH26 0QB, U.K.

D. L. Slusher, Department of Chemistry and Physics, Coastal Carolina University, P.O. Box 261954, Conway, SC 29528, USA.

J. P. Sparks, Department of Ecology and Evolutionary Biology, Cornell University, Corson Hall, Ithaca, NY 14853, USA.